



# Fermi National Accelerator Laboratory

FN-364  
1502.000

PRODUCTION OF ELECTRONS AND POSITRONS BY IMPINGING  
100 GeV PROTONS ON A TARGET FOR PURPOSE OF FILLING  
AN ELECTRON STORAGE RING

S. Conetti  
Institute for Particle Physics, Montreal, Canada

and

A. G. Ruggiero  
Fermi National Accelerator Laboratory, Batavia, Illinois 60510

April 1982



Operated by Universities Research Association Inc. under contract with the United States Department of Energy

## I. Introduction

To avoid seriously limiting coherent instability and too much beam loading on the RF system, it is convenient to inject in an electron storage ring at as high an energy as possible, preferably at the same energy that the storage ring is supposed to operate when in the colliding-mode. This, though, would be very expensive and requires larger and more complex accelerators operating as injectors.

As an alternative we propose here an interesting idea (see V.I. Balbekov et al., Xth International Conference on High Energy Accelerators, Protvino, USSR, July 1977, Vol. I, p. 177) to produce pairs of electrons and positrons by impinging primary protons on a target. This idea works very well and it is mostly suited for the Fermilab electron-proton proposals. Indeed Fermilab has already available a large energy and intense proton beam as a source.

The scheme we propose is similar to the one to collect antiprotons (The Fermilab Antiproton Source Design Report, February 1982). The major differences are that it is much easier to collect electrons and positrons, the yield from a target being two orders of magnitude larger, and that with electrons there is automatically a "cooling" technique to collect them. This is done by the synchrotron radiation damping, a cooling system which is reliable, extremely fast and inexpensive.

The scheme is simple and it can be understood by inspecting Figure 1 which shows the Fermilab site with all the accelerators and storage rings that will exist at one time or another. Figure 2 gives a closer look at the region around D0 where Main Ring, Tevatron and the electron storage ring touch each other.

The proton beam is accelerated as usual to 100 GeV. At this energy there is a small flat-top to allow for some rf manipulations that will be described in the following section. When the beam is ready it is extracted in several pulses, each with about the length of the electron storage ring. The extraction occurs at C17. The proton beam is taken to a target where  $e^\pm$ -pairs are produced. A transport line takes the chosen charge ( $e^+$  or  $e^-$ ) down to the electron storage ring where the beam is injected and stored. After a period of three betatron damping times the beam has been "cooled" and now the next proton beam segment can be extracted from the Main Ring to produce more  $e^\pm$ -pairs. This is repeated until the Main Ring is empty, at which time the cycle repeats.

In section III we discuss the targeting of the proton beam and the capture of the  $e^\pm$ 's in the storage ring. In section IV we show in detail our yield calculations.

We took under consideration two cases. One is a 5 GeV storage ring proposed by Columbia University and the other is a 10 GeV storage ring (CHEER) proposed by a Canadian group. The relevant parameters for these two rings are summarized in Table I.

We make the assumption that the bunching of the electron beam in the storage ring and the bunching of the proton beam in the Tevatron are the same and that corresponds, for both cases, to one bunch every 7 RF buckets in the Tevatron at 53 MHz. It is convenient to prepare the proton beam before targeting to produce  $e^\pm$ -beam already at the required bunching. Moreover, the bunching of one bunch every 7 RF buckets, corresponds to a beam gap of 130 nsec that can be used for the fall-off time of an extraction kicker in the Tevatron or a rise-time of an injection magnet in the electron storage ring.

We found filling times for the required intensities that ranges between a few minutes to several tens of minutes. This is short enough to make the idea quite attractive especially for the positron beam production.

## II. Main Ring RF Manipulation and Preparation of the Proton Beam for Targeting

The Main Ring cycle is shown in Figure 3. The Main Ring is filled-up as usual, in the box-car fashion at 8.0 GeV, with 13 Booster batches, for a total of  $3 \times 10^{13}$  protons. The beam is bunched with the standard 53.1 MHz,  $h=1113$ , RF system.

Before acceleration, three consecutive bunches every seven are eliminated with the fast, transverse super-damper as shown in Figure 4. This is a conventional technique at Fermilab.

The beam is then accelerated to 100 GeV where the cycle has a flat-top 0.3 sec. long.

We assume that each bunch, with careful adjustment of injection and transition energy crossing, has a longitudinal phase space area of 0.2 eV-sec and  $3 \times 10^{10}$  particles. The beam is made of a total of  $1.7 \times 10^{13}$  protons.

During flat-top the beam will undergo two major RF manipulations similar to those that have already been proposed for the Fermilab  $\bar{p}$  source.

### Phase I

At the end of the acceleration the beam is kept bunched by stationary buckets produced by the 4 MV, 53 MHz RF system. As first step the RF

voltage will be turned off slowly so that the beam will adiabatically debunch. It takes about 10 msec to do this, which corresponds to two phase oscillations at 4 MV/turn.

It is not possible to turn the RF off completely to zero, because of multipactoring problems and beam loading. The minimum voltage that can be reached is probably 10 kV, so the beam will not be completely debunched but will extend over  $\pm 180^\circ$  as shown in Figure 5. Bunches will touch each other.

At this stage it is proper to approximate four consecutive bunches as a single one with rectangular shape. The longitudinal phase space area of this larger bunch is

$$S = \frac{\pi}{2} \times 4 \times 0.2 \approx 1.3 \text{ eV-sec}$$

Each superbunch has  $1.2 \times 10^{11}$  protons, the length

$$\sigma_\tau = \pm 38 \text{ nsec}$$

and the height

$$\Delta E = \pm 8.6 \text{ MeV}$$

At this point the voltage of a 7.586 MHz RF system is turned on as quickly

as one can, say within one turn, that is 20  $\mu$ sec. This RF system corresponds to the harmonic number  $h=1113/7 = 159$  and creates stationary buckets to capture the superbunches as shown at the bottom of Figure 5.

Since the shape of the superbunches is mismatched to the trajectories of the  $h=159$  stationary buckets, the superbunches will rotate as shown in Figure 6.

We require that after a quarter of the phase oscillation the beam has a maximum energy spread

$$\frac{\Delta E}{E} = \pm 0.1\%$$

that is  $\Delta E = \pm 101$  MeV, and a bunch length

$$\sigma_T = \pm 3.2 \text{ nsec}$$

The required bucket height is

$$\Delta E_b = \sqrt{2} \Delta E = \pm 143 \text{ MeV}$$

which corresponds to the RF voltage

$$V = 140 \text{ kV}$$

at 7.586 MHz.

The bunch rotation takes a quarter of phase oscillation, that is about 20 msec.

As soon as the bunch rotation is accomplished one switches immediately to the 53 MHz RF system again. The 7.6 MHz is turned off at the same time the 53 MHz RF system is turned on, that is within one period (20  $\mu$ sec).

We require the voltage is set so that the shape of the bunch is matched to the new 53 MHz stationary bucket to stop the rotation of the bunches. For this purpose the bucket height

$$\Delta E_b = \frac{\Delta E}{\sin \phi/2}$$

where  $\Delta E = \pm 101$  MeV is the beam height and

$\phi = \pm 180^\circ \times 3.2$  nsec / 9.4 nsec =  $\pm 61^\circ$  the bunch extension:

$$\Delta E_b = 200 \text{ MeV}$$

This corresponds to a voltage  $V = 1.9$  MV at 53 MHz. At the end of this phase one has about 150 superbunches occupying one out of seven of the 53 MHz RF stationary buckets. Bunches are separated by about 130 nsec, have a longitudinal phase space area of 1.3 eV-sec and  $1.2 \times 10^{11}$  protons each.

The RF manipulation we have described above has also been proposed to combine 4 Main Ring bunches in one single superbunch for proton-antiproton collision in the Tevatron. Computer simulations to check the scheme exist

(K. Takayama, J. MacLachlan) and a preliminary experiment has already been tried successfully (J. Griffin and J. MacLachlan).

### Phase II

For targeting it is important to make the proton bunches as narrow as possible so that also the  $e^\pm$ -bunches are narrow enough to match the RF buckets in the electron storage ring.

The following RF manipulation has also been proposed for targeting protons to produce antiprotons (Fermilab, 1982 Antiproton Source Design).

The 53 MHz voltage is turned down slowly until bunches extend over  $\pm 90^\circ$ . The voltage is turned down in 13 msec, which corresponds to two phase oscillations with 1.9 MV/turn. In the following we shall assume the bunches have elliptical shape. At the end of the adiabatic voltage drop:

$$V = 750 \text{ kV}$$

$$\Delta E = \pm 88 \text{ MeV}$$

$$\sigma_T = \pm 4.7 \text{ nsec}$$

The bunch shape is continuously matched to the trajectories of the RF bucket.

Suddenly the voltage is turned on to full value (4 MV) within one turn ( $\sim 20 \mu\text{sec}$ ). We want to point out that RF voltage modulation at this proposed rate has already been demonstrated experimentally for the Main Ring. The bunch is now mismatched and will rotate in the similar fashion as illustrated in Figure 6.

At 4 MV/turn the bucket height is

$$E_b = \pm 290 \text{ MeV}$$

and the beam height after a quarter of phase oscillation (which lasts 1.3 msec) is

$$E = \pm 205 \text{ MeV}$$

which corresponds to a new length

$$\sigma_\tau = \pm 2.0 \text{ nsec}$$

The result depends on the individual bunch area before any RF manipulation is applied, here assumed to be 0.2 eV-sec. The final bunch length could be a factor of two smaller ( $\pm 1.0 \text{ nsec}$ ) if the bunch area were also a factor of two smaller at the start (0.1 eV-sec).

Right after a quarter of the phase oscillation has been completed and the beam bunches are the narrowest, a segment of the beam is extracted, targeted to produce the same number of  $e^\pm$ -bunches spaced by 130 nsec and injected in the electron storage ring in one single turn.

The bunches remaining in the Main Ring will continue to rotate for another quarter of phase oscillation, until they extend again over a phase

of  $\pm 90^\circ$ . At this time the RF voltage is dropped again, and very fast, to 750 kV.

As we have seen at this level, the bunches are matched and stop rotating. The beam in the Main Ring is kept under these conditions as long as necessary, until the e-bunches in the electron storage ring have been "cooled" enough in all directions by the synchrotron radiation. Typically this takes three betatron damping times, that is a total period of time that can range from 10 to 50 msec depending on the energy and the size of the electron storage ring.

When a new segment is ready for extraction and targeting the bunch rotation of phase II is repeated again. This will go on until the Main Ring is empty.

The length of the flat-top in the MR cycle is calculated as the sum of the duration of the steps we have described above:

$$t_{\text{flat-top}} = 10 \text{ msec} + 20 \text{ msec} + 15 \text{ msec} + (n-1)(3\tau_{\text{damping}})$$

where  $n$  is the number of pulses injected in the electron storage ring per Main Ring cycle. For the two rings shown in Table I we have at most  $t_{\text{flat-top}} = 0.23$  sec. Therefore a Main Ring cycle of 3.0 seconds sounds more than reasonable.

Finally observe that although extraction from the Main Ring at 100 GeV with a beam gap of 130 nsec appears to be possible, we did not investigate the requirements it would impose upon the whole extraction system.

### III. Proton Target and Electron Capture

At 100 GeV the proton emittance is  $\epsilon_H = \epsilon_V = 0.223\pi 10^{-6}$  m, which include, 95% of the beam with bi-gaussian distribution.

The proton beam can be focused on a target where  $\beta_H^* = \beta_V^* = 1$  m so that the rms beam spot size is

$$\sigma_H = \sigma_V = 0.193 \text{ mm}$$

To avoid onset of shock waves that could result in the density depletion of the target the energy-density deposition should be of no more than 200 J/g. With the beams cross section specified above the maximum number of protons that one can impinge on the target at one time is

$$N_p = 7.8 \times 10^{11}$$

for a target 5 cm long (see the Fermilab Antiproton Source Design Report).

The target we are actually considering here for  $e^\pm$ -pair production will be several times longer (40 cm) and therefore we should be capable to impinge on the target a number of protons in excess of  $10^{12}$ . As we can see from Table I, the actual number of protons hitting the target during one pulse does not exceed  $10^{12}$ , so that our choice of  $\beta_H^* = \beta_V^* = 1$  m is reasonable.

As a collector we can use a lithium lens similar to the one proposed for the antiproton collection. With this lens one can focus on a plane in

the target where  $\beta_H^* = \beta_V^* = 10$  cm for the electrons.

The maximum number of electrons (positrons) that can be captured depends eventually on the momentum aperture and betatron acceptance of the storage ring, that we estimate here to be about

$$\frac{\Delta p}{p} = \pm 1\%$$

$$A_H = A_V = 20\pi 10^{-6} \text{ m}$$

With a  $\beta^*=10$  cm this corresponds to a beam size of  $\pm 1.5$  mm and an angle of  $\pm 15$  mrad at the focal plane, assuming there zero dispersion.

Each electron bunch accepted will have therefore a momentum spread of  $\pm 1\%$  with a roughly uniform distribution and a longitudinal gaussian distribution of the same width as proton bunches. As we have seen in the previous section the width for 95% of the beam is  $\pm 2$  nsec.

Nevertheless only those electrons that will fall in the moving buckets created by the RF cavities in the storage ring will be captured. The bucket height and length are given in Table I. It turns out that the Columbia storage ring can capture considerably more electrons because, due to the RF choice, the buckets are longer and wider.

We estimate that only about 20% of the electrons will be RF captured for CHEER but as much 50% will be captured in the Columbia storage ring.

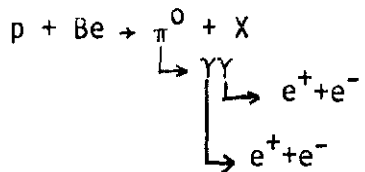
After three damping times of the betatron oscillations the injected beam is "cooled" to the equilibrium values which are shown also in Table I. These values are considerably smaller than those at the injection and there

is plenty of room for injection of subsequent pulses.

#### IV. Yield Calculations

We have prepared a Monte Carlo computer simulation to estimate the yield of electron and positron pairs produced by protons on a target.

The chain of reaction we have considered is the following:



In order to maximize the acceptance of the electron transport line, we propose to use the same target both for producing the  $\pi^0$ 's and to convert the photons. Given the ratio of momenta of the incoming protons and outgoing electrons (100 vs 5 or 10 GeV), it is important not to let the  $e^-$  electromagnetic shower grow, so as not to degrade the electron's momenta. For these reasons we choose a beryllium target (absorption length  $\sim$  radiation length) 40 cm long and wide enough so that particles do not escape radially. A more detailed study would be required to determine the optimum target length, but our simple minded Monte Carlo showed the value of 40 cm to be quite reasonable.

(i) The initial conditions for the proton beam are first generated. We generate a proton by assigning four coordinate variables

$x, x'$  and  $y, y'$

taken randomly according to a gaussian distribution in any of the four variables with zero means and standard deviation values given by

$$\sigma_x = \sqrt{\epsilon \beta_x^*}$$

$$\sigma_y = \sqrt{\epsilon \beta_y^*}$$

$$\sigma_{x'} = \sqrt{\epsilon / \beta_x^*}$$

$$\sigma_{y'} = \sqrt{\epsilon / \beta_y^*}$$

with  $\epsilon = 3.72 \times 10^{-8}$  m the rms emittance, and  $\beta_x^* = \beta_y^* = 1$  m the lattice values at the focus which is assumed at the center of the target. At the focus there is a waist, that is  $\beta_x' = \beta_y' = 0$ . The initial conditions generated correspond to the location of the focus but then the actual initial coordinates at the beginning of the target ( $s=0$ ) are calculated by a single transposition

$$x + x' - x' l/2$$

$$y + y' - y' l/2$$

$$x' \rightarrow x'$$

$$y' \rightarrow y'$$

and the angles,  $x', y'$  are unchanged.

The distributions of the particles so generated at the focus location are shown in Figures 7, 8, 9, and 10. Note that these, as well as the

following figures represent the result of generating 10,000 protons.

The dispersion at the focus is zero and the protons have been generated all with the same momentum.

(ii) Protons are made to interact in the target with an exponential distribution  $e^{-s/\lambda}$ ,  $\lambda=36.7$  cm (Fig. 11). Only primary interactions are taken into account, so that the final electron/positron yield will be somewhat underestimated, since we are not keeping track of  $\pi^0$ 's generated in secondary interactions.

A parameterization for the longitudinal and transversal momentum distributions of the production  $\pi^0$ 's was obtained by averaging the  $\pi^+$  and  $\pi^-$  production data, as measured in the bubble chamber. Such a choice was motivated by the fact that better data exists for the charged than for the neutral  $\pi$ 's over the kinematical region of more copious production. Again this approximation will lead to a certain underestimate of the final yield, since photons originated from  $\eta$  production and decay are neglected.

The parameterization employed was obtained from the 200 GeV data of Kafha et al., Phys. Rev. D16, 1977, 1261 and one of the form ( $X_F$  being the scaling variable  $p\bar{t}/p_{\max}^*$ )

$$E \frac{d\sigma}{dX_F} \sim e^{-(B|X_F| + C|X_F|^2)} \quad (1)$$

$$\begin{aligned} \text{with } B &= 4.35 \\ C &= 4.50 \end{aligned}$$

and

$$\frac{d\sigma}{dp_{\perp}^2} \sim e^{-6p_{\perp}^2} \quad (2)$$

Although it is known that the transverse momentum distribution is not completely independent of  $X_F$ , the variations over the region of interest are small enough that the use of a factorized expression gives a very reasonable approximation. Comparison with data measured at 100 and 400 GeV (C. Bromberg et al., Nucl. Phys. B, 107, 1976, 82) guaranteed the validity of scaling in the  $X_F$  and  $p$  variables, making legitimate the use of the parameterization obtained at 200 GeV.

The results of R.D. Kass et al., Phys. Rev. D20, 1979, 605 were used to obtain the average  $\pi^0$  multiplicity, which is measured to be equal to 3 at 100 GeV.

Operationally, for each interacting proton three  $\pi^0$ 's were generated: for each  $\pi^0$  a value of  $-1 < X_F < 1$  was chosen by sampling the distribution (1); next a value for  $p$  distributed according to (2) was obtained in the range  $0 < p < p^{***} = (s/2)\sqrt{1-X_F^2}$ . The azimuthal angle was then thrown with a flat probability.

The distribution of the  $\pi^0$ 's in the four-dimensional phase space  $(x, x', y, y')$  is shown in Figures 12, 13, 14, and 15.

The momentum distribution of the  $\pi^0$ 's is shown in Figure 16.

(iii) The  $\pi^0$  mesons are made to decay immediately in a pair of  $\gamma$ 's. The decay distribution is obtained by picking at random the center of mass decay angle  $\theta_{\pi}$ . Lorentz transformations yield for the lab momenta of the two gammas

$$p_1 = \frac{1}{2} m_\pi c \gamma (1 + \beta_\pi \cos\theta)$$

$$p_2 = \frac{1}{2} m_\pi c \gamma (1 - \beta_\pi \cos\theta)$$

and for the respective angles of production from the direction of motion of the  $\pi^0$

$$\theta_1 = \arcsin \left( \frac{m_\pi c}{2p_1} \sin \theta_\pi \right)$$

$$\theta_2 = - \arcsin \left( \frac{m_\pi c}{2p_2} \sin \theta_\pi \right)$$

The azimuthal angle is also generated randomly.

The distribution of the first gamma in  $x', y'$  and momentum ( $p_1$ ) is shown in Figures 17, 18, and 19. The data for the second gamma are shown in Figures 20, 21, and 22. The distribution in  $x$  and  $y$ , of course, are the same as the  $\pi^0$ 's.

(iv) The gammas so generated will travel down the target and then will convert in pairs of  $e^+e^-$ .

We have used conversion length of 45.4 cm. The distribution of the coordinate for the gamma conversion is given in Figure 23. The distribution of the  $x, x', y, y'$  coordinates at the moment of conversion are

shown in Figures 24, 25, 26, and 27. The momenta of the electrons are obtained from a flat momentum distribution and consequently the positron momentum is derived from

$$p_{e^+} + p_{e^-} = p_\gamma$$

The opening angle of the produced pairs, being of the order of  $m_e/E_e$  is neglected, so that the pair is produced with the same direction of motion of the converting gamma. The momentum of the electrons and positrons at production is given in Figures 28 and 29 respectively.

Finally, the  $e^\pm$  have a chance by traveling down the remaining part of the target to loose some amount of energy by bremsstrahlung. Figures 30 and 31 show the distribution of the coordinate where radiation occurs. We have assumed a radiation length of 35.3 cm. The energy lost is chosen according to a  $1/E$  distribution. The final momentum distribution is given in Figures 32 and 33.

(v) We assume that a collector lens is located beyond the target. The focal plane of the collector is taken to be 15 cm downstream from the beginning of the target. The distributions of the electrons and positrons in the  $(x, x')$  and  $(y, y')$  planes projected back at the focal plane are shown in Figures 34, 35, 36, and 37. The characteristic butterfly shape is easily recognized.

The diagrams given in Figures 38, 39, 40, 41 and in Figures 42, 43, 44, 45 show the phase space distribution for  $e^+$  at the desired momenta of 5

and 10 GeV ( $\pm 5\%$ ) respectively.

In these diagrams we have outlined an ellipse with semi-axis of 1.45 mm and 14.5 mrad which corresponds to an acceptance  $20\pi$  mm-mrad in both planes.

The yield for a  $20\pi$  mm-mrad acceptance in both planes and  $\pm 5\%$  momentum bite is attained by dividing the total number of particles falling within the ellipse by 10,000, the number of protons generated in our Monte Carlo simulation. In Table I we give the yield for  $\pm 1\%$  momentum bite. As one can see, two minutes are required to fill up a 5 GeV electron storage ring as proposed by Columbia University. On the other hand, CHEER, the 10 GeV Canadian proposed ring would take about an hour. Nevertheless the betatron acceptance in CHEER is much larger than considered here and is capable of capturing more electrons, provided the RF frequency is lowered from 804 MHz to 496 MHz. In this case, the filling time could be less than ten minutes.

Table I. Comparison Between Two Different Energy Cases

	<u>CHEER</u>	<u>Columbia</u>
Energy, GeV	10	5
Radius, m	283.0	56.6
RF Frequency, MHz	804	496
RF Peak Voltage, MV	24.8	6.0
Energy Loss, MeV/turn	9.66	3.51
Momentum Compaction Factor, $\alpha$	0.00583	0.00250
No. of Bunches	45	9 (21)
No. of Electr./Bunch	$10^{11}$	$0.58 \times 10^{11}$
Bucket Height, $\Delta p/p$	$\pm 0.51\%$	$\pm 1.15\%$
Bucket Length, nsec	0.73	0.97
Harmonic No.	4770	588
$\sin \phi_s$	0.390	0.585
Betatron Damping Time, msec	12.2	3.7
rms Bunch Length, nsec	0.03	0.05
rms Bunch Energy Spread	0.085%	0.1%
rms Betatron Emittance with Full Coupling, $10^{-6}$ m	0.025	0.065
No. of Proton Pulses per MR Cycle	4	18
MR Flat Top Length, msec	145	225
No. of protons per pulse on the target	$7.7 \times 10^{11}$	$1.53 \times 10^{11}$
Fraction of electrons captured within an acceptance of $20\pi$ mm-mrad and $\Delta E/E = \pm 1\%$	0.2	0.5
Yield: $N_e / N_p$	$2.3 \times 10^{-4}$	$9.2 \times 10^{-4}$
Filling Time with a MR Cycle of 3 sec.	3,450 sec	100 sec

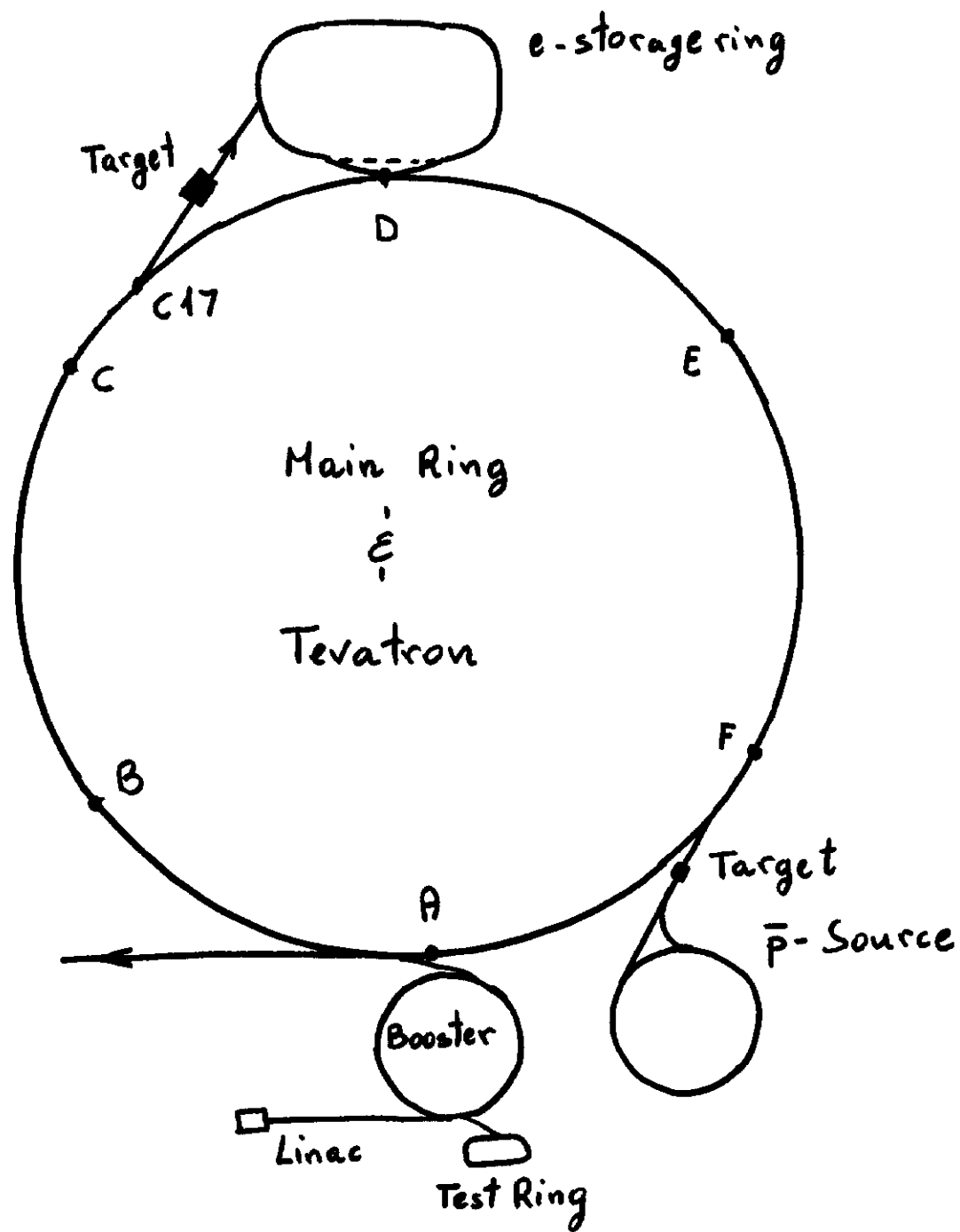


Fig. 1. Plan View of Fermilab Site

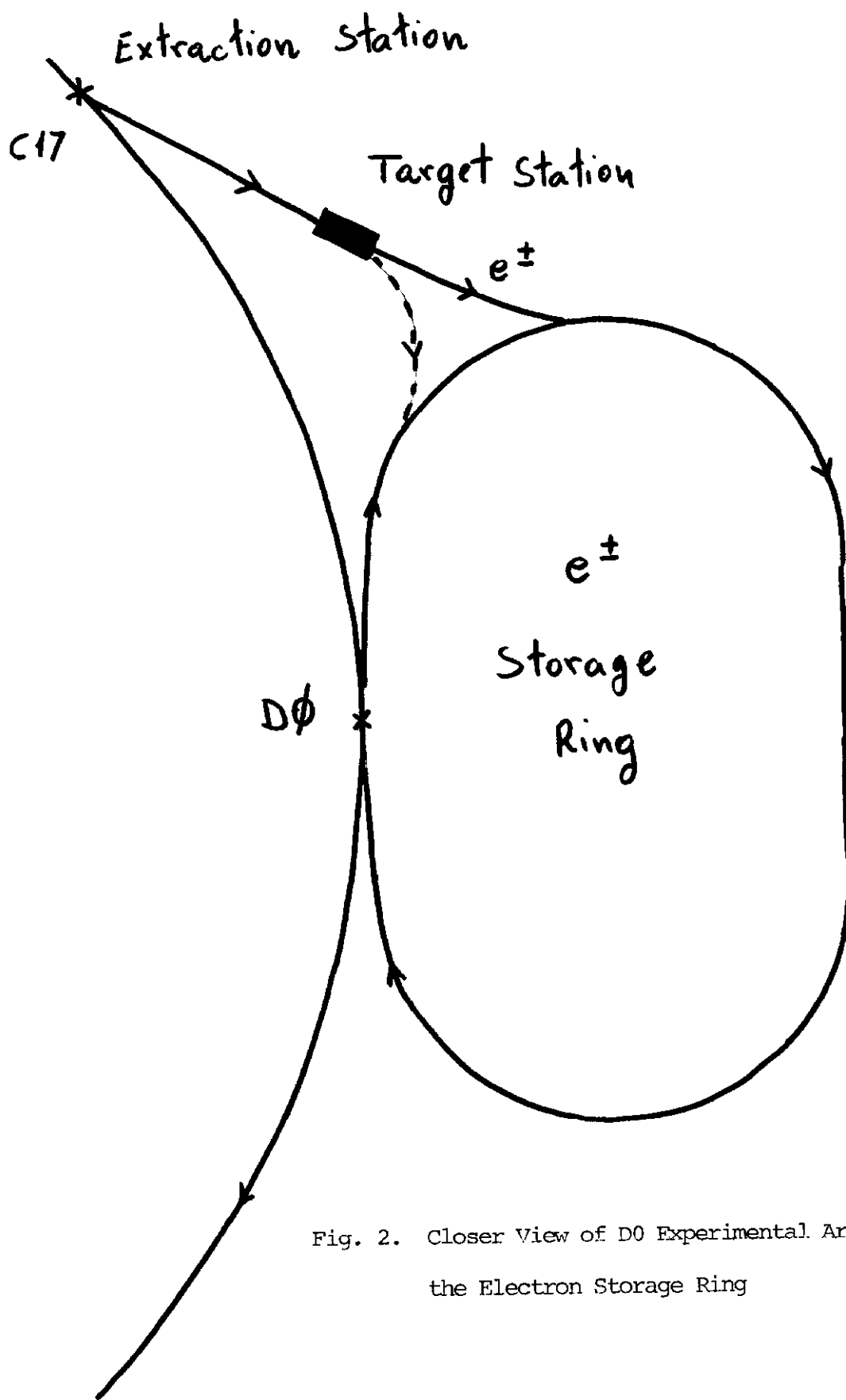


Fig. 2. Closer View of D0 Experimental Area with  
the Electron Storage Ring

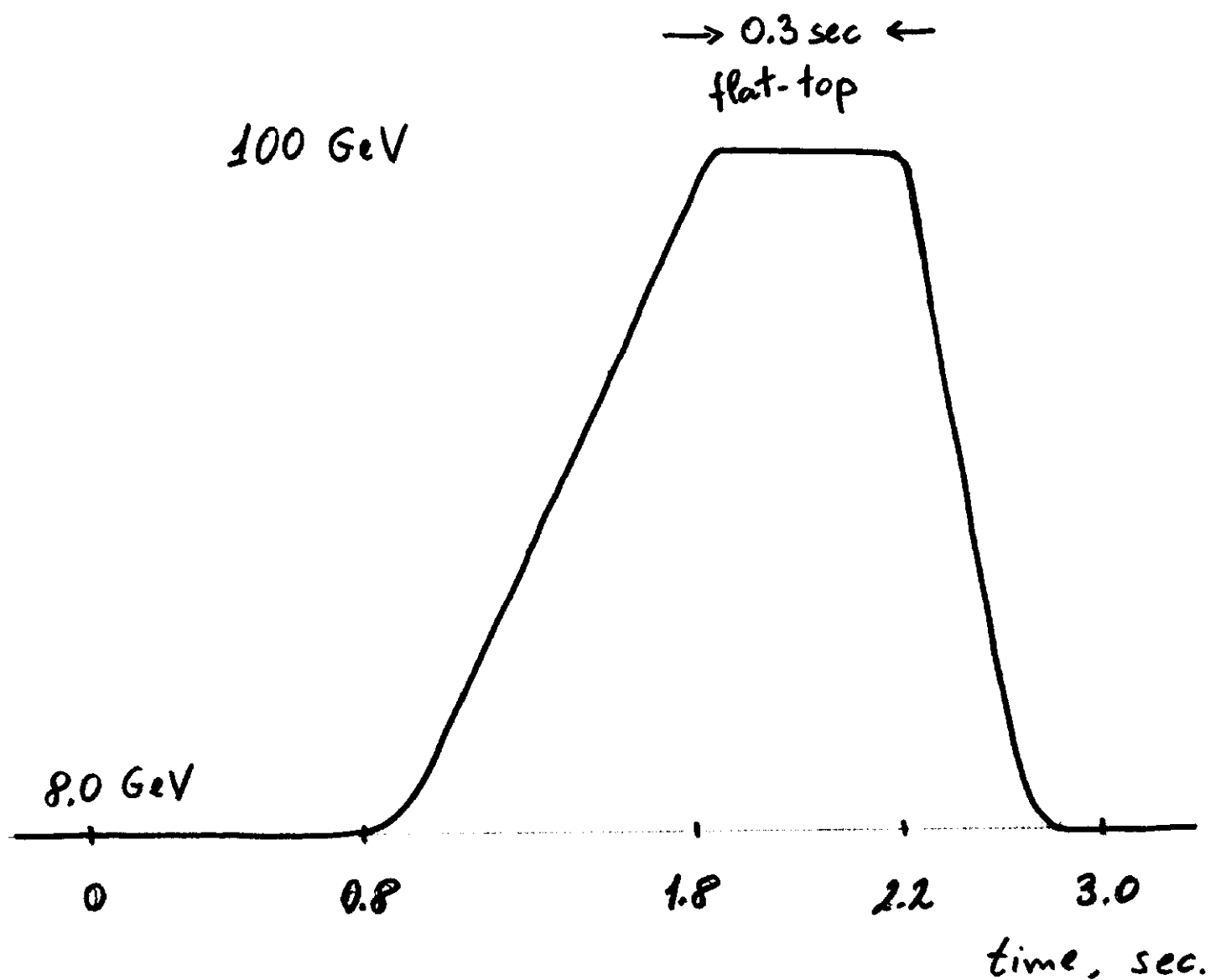


Fig. 3. Diagram of the Main Ring Cycle

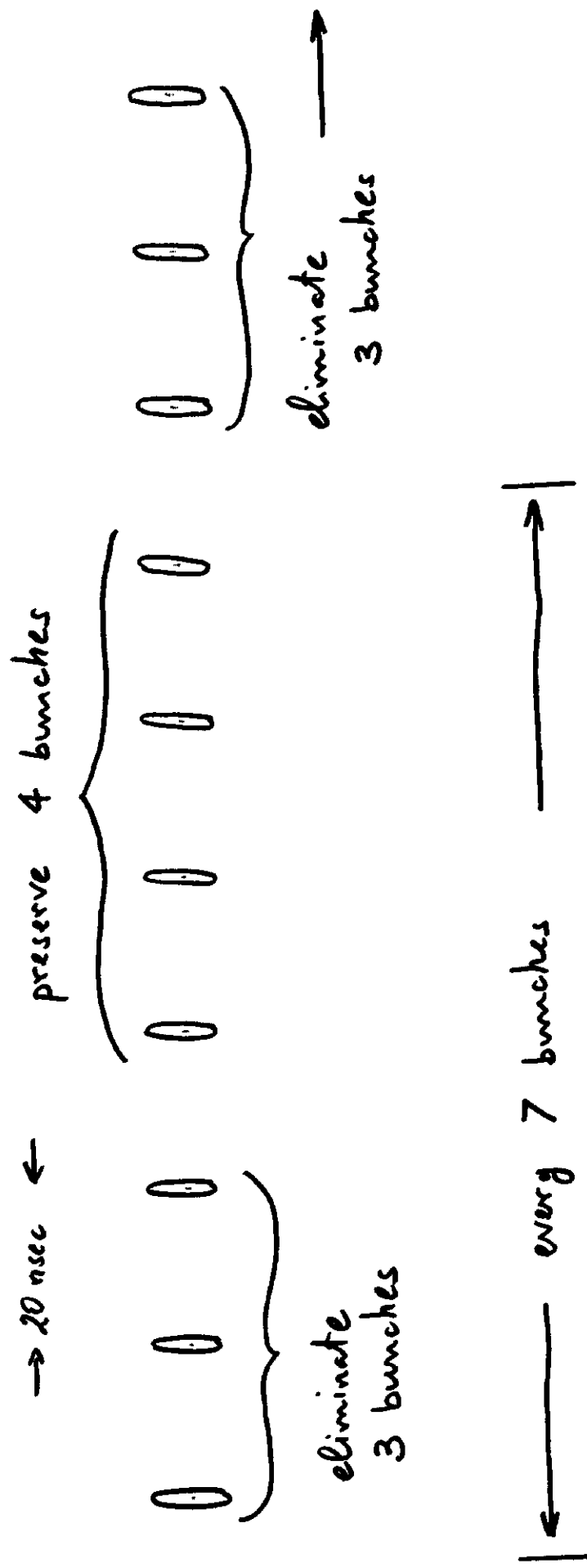


Fig. 4. Proton Beam Bunching in the Main Ring at 8.0 GeV

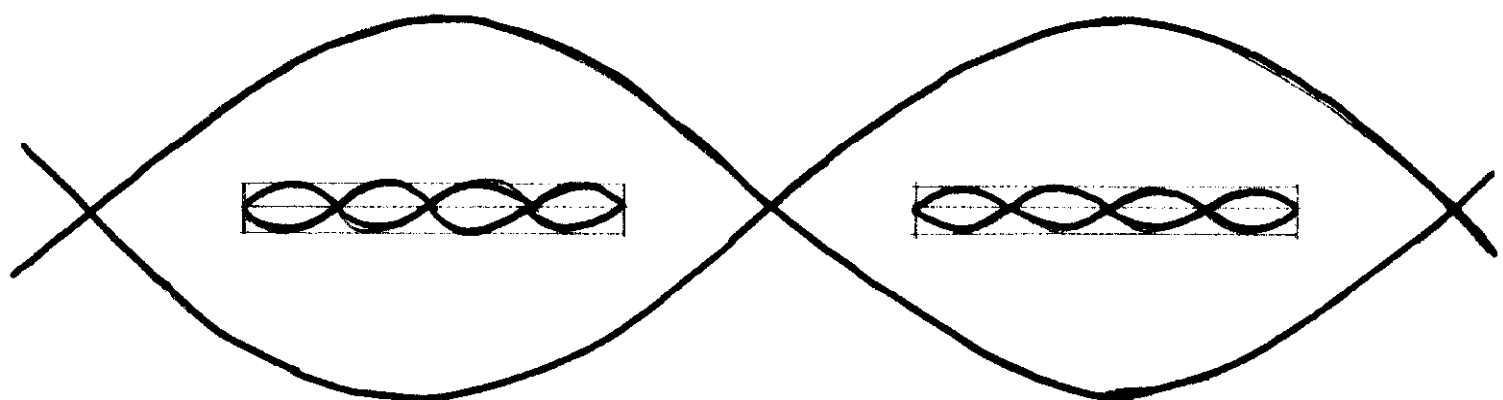


Fig. 5. Creation of the Proton Superbunches in the Main Ring

$V = 1.9 \text{ MV}$  @  $53 \text{ MHz}$

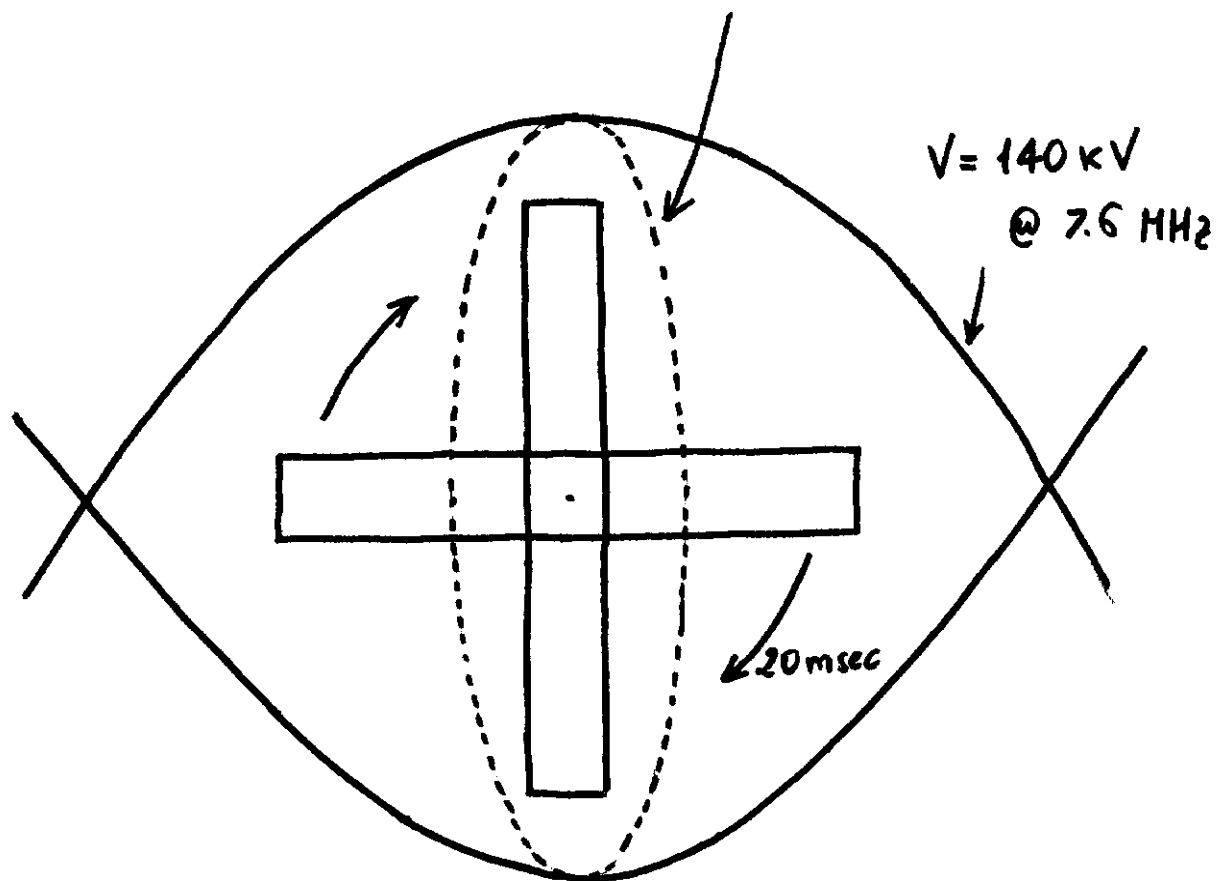


Fig. 6. Bunch Rotation at  $h = 159$  in the Main Ring









S OF 1ST INTERACTION  
H300K ID = 3

DATE 82/04/13

NO = 5

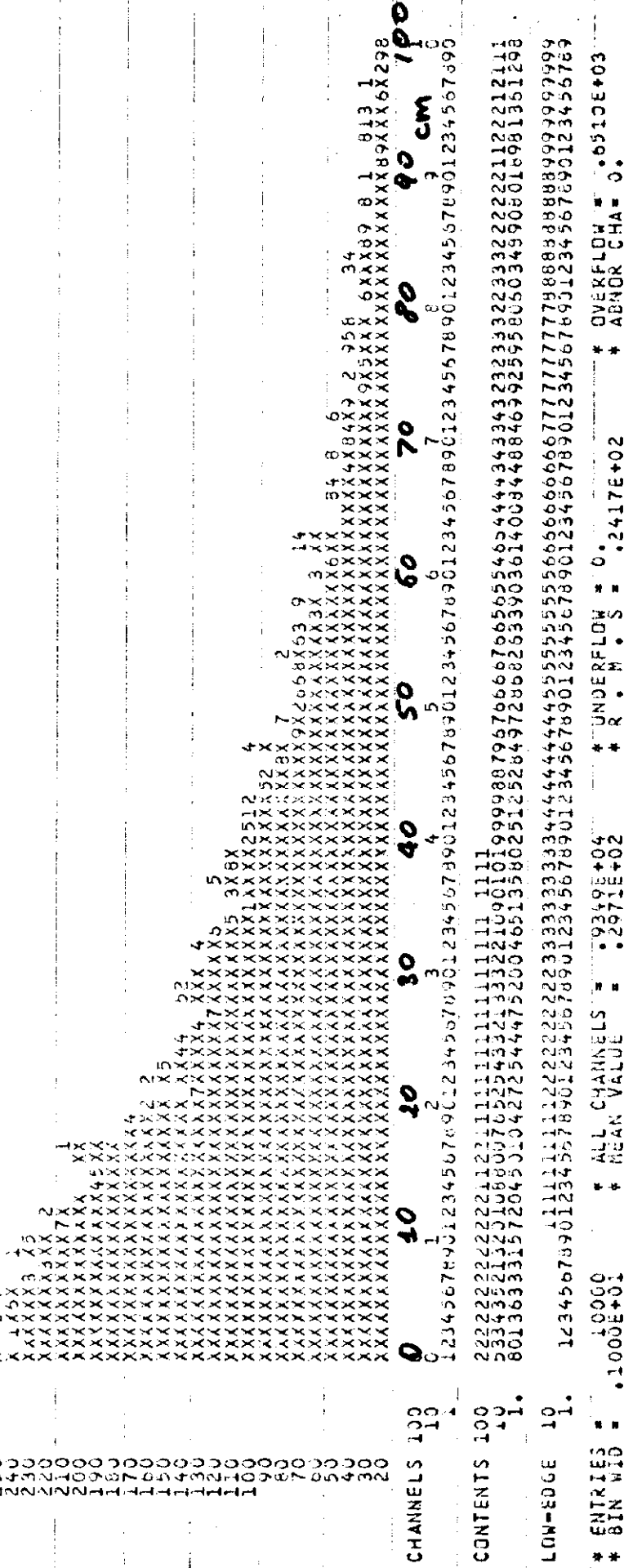


Fig. 11. Distribution of the Decay Distances of the Protons in  $\pi^0$ 's

PIZERO X  
HBOOK

1

23

6  
•  
0  
n

DATE 62/04/13

906

4

Fig. 12.  $\pi^0$  x - Distribution at the moment of production

PIZER & CO.

3000K 10 = 7

DATE 62/04/13

1  
2

A decorative horizontal border consisting of a repeating pattern of the letter 'X'. The pattern is formed by two thin black lines crossing each other at regular intervals.

סימן כוכב

```

ENTRIES = 19896 * ALL CHANNELS = .5529E+04 * UNDERFLOW = .7170E+04
BIN WIDTH = .3003E+00 * MEAN VALUE = .2717E-02 * OVERFLOW = .7205E+04

```

Fig. 13.  $\pi^0$  - Distribution at the moment of production

PIZERO  
HBOOK

DATE 82/04/13

NO = 8

840

820

800

780

760

740

720

700

680

660

640

620

600

580

560

540

520

500

480

460

440

420

400

380

360

340

320

300

280

260

240

220

200

180

160

140

120

100

80

60

40

20

0

16

32

64

128

256

512

1024

2048

4096

8192

16384

32768

65536

131072

262144

524288

1048576

2097152

4194304

8388608

16777216

33554432

67108864

134117732

26823544

53647088

107294176

214588352

429176704

858353408

1716706816

3433413632

6866827264

1373365456

2746730912

5493461824

1098692168

2197384336

4394768672

8789537344

1757874488

3515748976

7031497952

1406295904

2812591808

5625983616

1125196723

2250393446

4500786892

9001573784

1800314552

3600629104

7201258208

14402516416

28805032832

57610065664

1152201332

2304402664

4608805328

9217616656

1843523312

368706624

737413248

1474825616

2949651232

58992064

11798408

23596816

47193632

94387264

188774528

377549056

755098112

1510196224

302039248

604078496

1208156992

2416313984

4832627968

9665255936

1933051873

3866102746

7732205492

1546441084

3092882168

6185764336

1237152872

2474305744

4948611488

9897223976

1979446952

3958893904

7917787808

1583557616

3167115232

633443264

1267283296

2534566592

5068163184

1013633216

2027266688

4054433376

8108867352

1621773504

3243547008

6487094016

1295408832

2584817664

5169633264

1033936632

2067873328

4137767168

8275534336

1655106664

3310133328

6620263264

1324056640

2640112224

5280224448

1056444444

2111111111

4444444444

8888888888

1777777777

3333333333

6566566565

1444444444

2321111111

5362222222

110

10

9

8

7

6

5

4

3

2

1

0

CHANNELS 100

0

1

2

3

4

5

6

7

8

9

10

11

12

13

14

15

16

17

18

19

20

21

22

23

24

25

26

27

28

29

30

31

32

33

34

35

36

37

38

39

40

41

42

43

44

45

46

47

48

49

50

51

52

53

54

55

56

57

58

59

60

61

62

63

64

65

66

67

68

69

70

71

72

73

74

75

76

77

78

79

80

81

82

83

84

85

86

87

88

89

90

91

92

93

94

95

96

97

98

99

100

101

102

103

104

105

106

107

108

109

110

111

PIZERO Y<sup>1</sup>  
H3OCK ID \* 9

DATE 82/04/13 NO = 9

156  
152  
144  
139  
132  
123  
124  
120  
126  
104  
100  
96  
92  
88  
84  
80  
76  
72  
68  
64  
60  
56  
52  
48  
44  
40  
36  
32  
28  
24  
CHANNELS 199

0

1

2

3

4

5

6

7

8

9

10

11

12

13

14

15

16

17

18

19

20

21

22

23

24

25

26

27

28

29

30

31

32

33

34

35

36

37

38

39

40

41

42

43

44

45

46

47

48

49

50

51

52

53

54

55

56

57

58

59

60

61

62

63

64

65

66

67

68

69

70

71

72

73

74

75

76

77

78

79

80

81

82

83

84

85

86

87

88

89

90

91

92

93

94

95

96

97

98

99

100

101

102

103

104

105

106

107

108

109

110

111

112

113

114

115

116

117

118

119

120

121

122

123

124

125

126

127

128

129

130

131

132

133

134

135

136

137

138

139

140

141

142

143

144

145

146

147

148

149

150

151

152

153

154

155

156

157

158

159

160

161

162

163

164

165

166

167

168

169

170

171

172

173

174

175

176

177

178

179

180

181

182

183

184

185

186

187

188

189

190

191

192

193

194

195

196

197

198

199

200

201

202

203

204

205

206

207

208

209

210

211

212

213

214

215

216

217

218

219

220

221

222

223

224

225

226

227

228

229

221

222

223

224

225

226

227

228

229

221

222

223

224

225

226

227

228

229

221

222

223

224

225

226

227

228

229

221

222

223

224

225

226

227

228

229

221

222

223

224

225

226

227

228

229

221

222

223

224

225

226

227

228

229

221

222

223

224

225

226



GAMMA X#

HBOOK ID # 11

DATE 82/04/13

NO = 11

127.5

125

122.5

120.5

117.5

115

112.5

110.5

107.5

105

102.5

99.5

97.5

95

92.5

90

87.5

85

82.5

80

77.5

75

72.5

70

67.5

65

62.5

60

57.5

55

52.5

50

47.5

45

42.5

40

37.5

35

32.5

30

27.5

CHANNELS 100

0

1

2

3

4

5

6

7

8

9

10

11

12

13

14

15

16

17

18

19

20

21

22

23

24

25

26

27

28

29

30

31

32

33

34

35

36

37

38

39

40

41

42

43

44

45

46

47

48

49

50

51

52

53

54

55

56

57

58

59

60

61

62

63

64

65

66

67

68

69

70

71

72

73

74

75

76

77

78

79

80

81

82

83

84

85

86

87

88

89

90

91

92

93

94

95

96

97

98

99

100

CONTENTS 100  
101  
102  
103  
104  
105  
106  
107  
108  
109  
110  
111  
112  
113  
114  
115  
116  
117  
118  
119  
120  
121  
122  
123  
124  
125  
126  
127  
128  
129  
130  
131  
132  
133  
134  
135  
136  
137  
138  
139  
140  
141  
142  
143  
144  
145  
146  
147  
148  
149  
150  
151  
152  
153  
154  
155  
156  
157  
158  
159  
160  
161  
162  
163  
164  
165  
166  
167  
168  
169  
170  
171  
172  
173  
174  
175  
176  
177  
178  
179  
180  
181  
182  
183  
184  
185  
186  
187  
188  
189  
190  
191  
192  
193  
194  
195  
196  
197  
198  
199  
200  
201  
202  
203  
204  
205  
206  
207  
208  
209  
210  
211  
212  
213  
214  
215  
216  
217  
218  
219  
220  
221  
222  
223  
224  
225  
226  
227  
228  
229  
230  
231  
232  
233  
234  
235  
236  
237  
238  
239  
240  
241  
242  
243  
244  
245  
246  
247  
248  
249  
250  
251  
252  
253  
254  
255  
256  
257  
258  
259  
260  
261  
262  
263  
264  
265  
266  
267  
268  
269  
270  
271  
272  
273  
274  
275  
276  
277  
278  
279  
280  
281  
282  
283  
284  
285  
286  
287  
288  
289  
290  
291  
292  
293  
294  
295  
296  
297  
298  
299  
300  
301  
302  
303  
304  
305  
306  
307  
308  
309  
310  
311  
312  
313  
314  
315  
316  
317  
318  
319  
320  
321  
322  
323  
324  
325  
326  
327  
328  
329  
330  
331  
332  
333  
334  
335  
336  
337  
338  
339  
3310  
3311  
3312  
3313  
3314  
3315  
3316  
3317  
3318  
3319  
33100  
33101  
33102  
33103  
33104  
33105  
33106  
33107  
33108  
33109  
33110  
33111  
33112  
33113  
33114  
33115  
33116  
33117  
33118  
33119  
331100  
331101  
331102  
331103  
331104  
331105  
331106  
331107  
331108  
331109  
331110  
331111  
331112  
331113  
331114  
331115  
331116  
331117  
331118  
331119  
3311100  
3311101  
3311102  
3311103  
3311104  
3311105  
3311106  
3311107  
3311108  
3311109  
3311110  
3311111  
3311112  
3311113  
3311114  
3311115  
3311116  
3311117  
3311118  
3311119  
33111100  
33111101  
33111102  
33111103  
33111104  
33111105  
33111106  
33111107  
33111108  
33111109  
33111110  
33111111  
33111112  
33111113  
33111114  
33111115  
33111116  
33111117  
33111118  
33111119  
331111100  
331111101  
331111102  
331111103  
331111104  
331111105  
331111106  
331111107  
331111108  
331111109  
331111110  
331111111  
331111112  
331111113  
331111114  
331111115  
331111116  
331111117  
331111118  
331111119  
3311111100  
3311111101  
3311111102  
3311111103  
3311111104  
3311111105  
3311111106  
3311111107  
3311111108  
3311111109  
3311111110  
3311111111  
3311111112  
3311111113  
3311111114  
3311111115  
3311111116  
3311111117  
3311111118  
3311111119  
33111111100  
33111111101  
33111111102  
33111111103  
33111111104  
33111111105  
33111111106  
33111111107  
33111111108  
33111111109  
33111111110  
33111111111  
33111111112  
33111111113  
33111111114  
33111111115  
33111111116  
33111111117  
33111111118  
33111111119  
331111111100  
331111111101  
331111111102  
331111111103  
331111111104  
331111111105  
331111111106  
331111111107  
331111111108  
331111111109  
331111111110  
331111111111  
331111111112  
331111111113  
331111111114  
331111111115  
331111111116  
331111111117  
331111111118  
331111111119  
3311111111100  
3311111111101  
3311111111102  
3311111111103  
3311111111104  
3311111111105  
3311111111106  
3311111111107  
3311111111108  
3311111111109  
3311111111110  
3311111111111  
3311111111112  
3311111111113  
3311111111114  
3311111111115  
3311111111116  
3311111111117  
3311111111118  
3311111111119  
33111111111100  
33111111111101  
33111111111102  
33111111111103  
33111111111104  
33111111111105  
33111111111106  
33111111111107  
33111111111108  
33111111111109  
33111111111110  
33111111111111  
33111111111112  
33111111111113  
33111111111114  
33111111111115  
33111111111116  
33111111111117  
33111111111118  
33111111111119  
331111111111100  
331111111111101  
331111111111102  
331111111111103  
331111111111104  
331111111111105  
331111111111106  
331111111111107  
331111111111108  
331111111111109  
331111111111110  
331111111111111  
331111111111112  
331111111111113  
331111111111114  
331111111111115  
331111111111116  
331111111111117  
331111111111118  
331111111111119  
3311111111111100  
3311111111111101  
3311111111111102  
3311111111111103  
3311111111111104  
3311111111111105  
3311111111111106  
3311111111111107  
3311111111111108  
3311111111111109  
3311111111111110  
3311111111111111  
3311111111111112  
3311111111111113  
3311111111111114  
3311111111111115  
3311111111111116  
3311111111111117  
3311111111111118  
3311111111111119  
33111111111111100  
33111111111111101  
33111111111111102  
33111111111111103  
33111111111111104  
33111111111111105  
33111111111111106  
33111111111111107  
33111111111111108  
33111111111111109  
33111111111111110  
33111111111111111  
33111111111111112  
33111111111111113  
33111111111111114  
33111111111111115  
33111111111111116  
33111111111111117  
33111111111111118  
33111111111111119  
331111111111111100  
331111111111111101  
331111111111111102  
331111111111111103  
331111111111111104  
331111111111111105  
331111111111111106  
331111111111111107  
331111111111111108  
331111111111111109  
331111111111111110  
331111111111111111  
331111111111111112  
331111111111111113  
331111111111111114  
331111111111111115  
331111111111111116  
331111111111111117  
331111111111111118  
331111111111111119  
3311111111111111100  
3311111111111111101  
3311111111111111102  
3311111111111111103  
3311111111111111104  
3311111111111111105  
3311111111111111106  
3311111111111111107  
3311111111111111108  
3311111111111111109  
3311111111111111110  
3311111111111111111  
3311111111111111112  
3311111111111111113  
3311111111111111114  
3311111111111111115  
3311111111111111116  
3311111111111111117  
3311111111111111118  
3311111111111111119  
33111111111111111100  
33111111111111111101  
33111111111111111102  
33111111111111111103  
33111111111111111104  
33111111111111111105  
33111111111111111106  
33111111111111111107  
33111111111111111108  
33111111111111111109  
33111111111111111110  
33111111111111111111  
33111111111111111112  
33111111111111111113  
33111111111111111114  
33111111111111111115  
33111111111111111116  
33111111111111111117  
33111111111111111118  
33111111111111111119  
331111111111111111100  
331111111111111111101  
331111111111111111102  
331111111111111111103  
331111111111111111104  
331111111111111111105  
331111111111111111106  
331111111111111111107  
331111111111111111108  
331111111111111111109  
331111111111111111110  
331111111111111111111  
331111111111111111112  
331111111111111111113  
331111111111111111114  
331111111111111111115  
331111111111111111116  
331111111111111111117  
331111111111111111118  
331111111111111111119  
3311111111111111111100  
3311111111111111111101  
3311111111111111111102  
3311111111111111111103  
3311111111111111111104  
3311111111111111111105  
3311111111111111111106  
3311111111111111111107  
3311111111111111111108  
3311111111111111111109  
3311111111111111111110  
3311111111111111111111  
3311111111111111111112  
3311111111111111111113  
3311111111111111111114  
3311111111111111111115  
3311111111111111111116  
3311111111111111111117  
3311111111111111111118  
33111111

GAMMA1 Y#

HBOOK ID

12

DATE 82/04/13

NO # 12

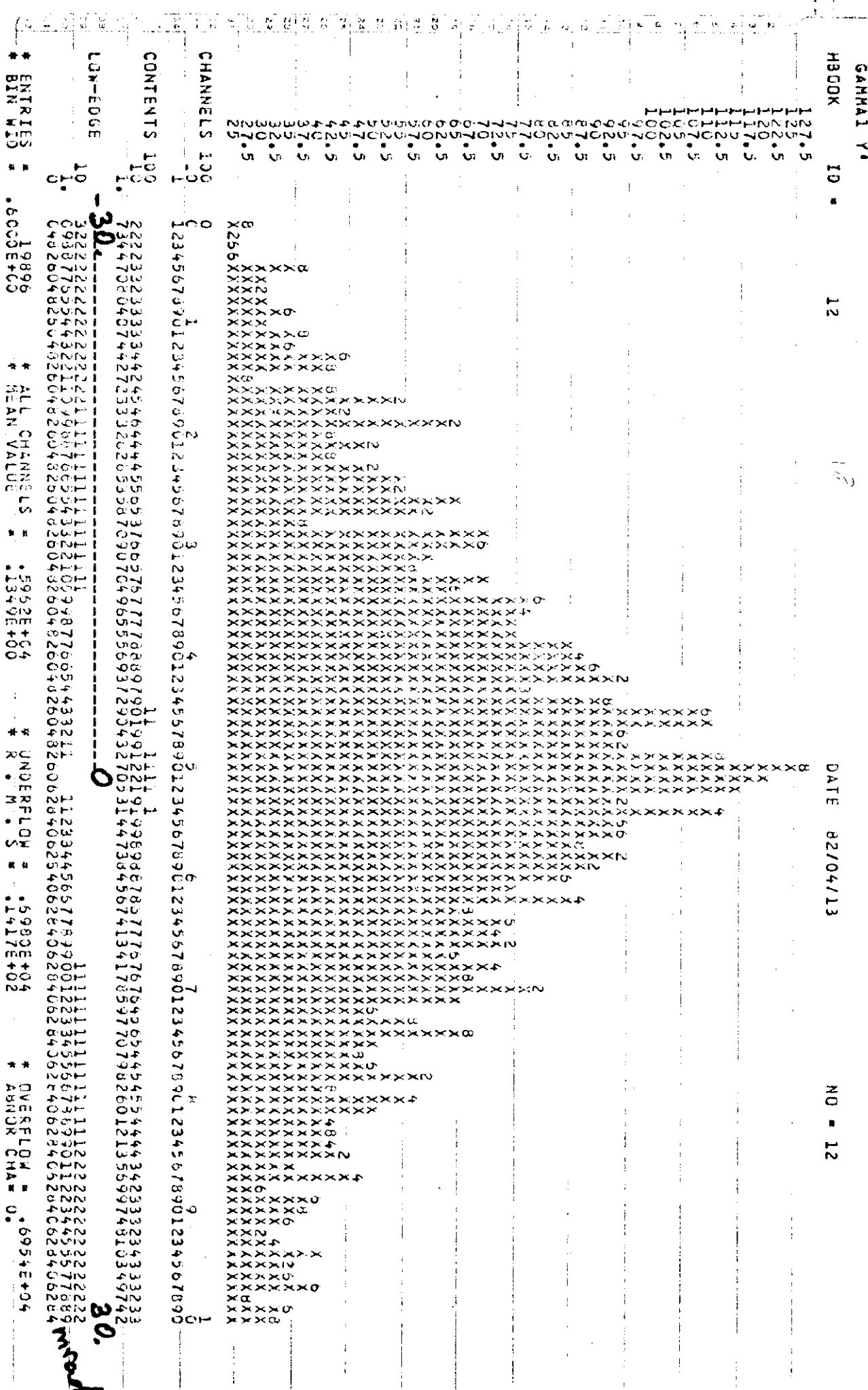


Fig. 18:  $\nu'$  - Distribution of gamma #1 at  $\bar{\kappa}^0$  decay

SAMAI MOMENTUM

13

DATE 82/04/13

M  
T  
I  
C  
Z

TANNINS 100

6

9

9

3

Fig. 19. Momentum Distribution of gamma #1 at  $\tau^0$  decay





SIGMA2 MOMENTUM  
4300K ID =

107.5
105.
102.5
100.
97.5
95.
92.5
90.
87.5
85.

DATE 82/04/13 NO = 16

4300K 10 =

DATE 82/04/13

NO. 11 = 16

The image shows a large grid of handwritten characters, mostly 'X's, arranged in a rectangular pattern. Interspersed among these 'X's are various numerical digits (1 through 9) and some other symbols like '+' and '-'. The grid is roughly 100 units wide and 100 units high. The handwriting is somewhat uniform but lacks a formal grid structure.

CHANNELS 100	10	P	1234	1
CONTENTS 100	10		10001	
	11		09900	
	11		5920	
LDM-EDGE 10	10		8888	1
	11		0134	
	11		0628	
	0		0	
				19
				* ENTRIES =

ONE L

INDIE  
88406  
58011  
11565  
05232  
22233  
90124

567 1 1 22  
9074 1 199001  
3406 \*

**24**  
90

Fig. 22. Momentum Distribution of gamma #2 at  $\pi^0$  decay

## SUF GAMMA CONVERSION

HBOOK 10 \* 17

DATE 82/04/13 NO = 17

1125

1160

1275

1250

1222

1023

975

920

900

875

849

825

800

775

750

700

675

650

625

600

575

550

525

500

475

450

425

400

375

350

325

300

275

250

225

200

175

150

125

100

75

50

25

0

1

2

3

4

5

6

7

8

9

0

1

2

3

4

5

6

7

8

9

0

1

2

3

4

5

6

7

8

9

0

1

2

3

4

5

6

7

8

9

0

1

2

3

4

5

6

7

8

9

0

1

2

3

4

5

6

7

8

9

0

1

2

3

4

5

6

7

8

9

0

1

2

3

4

5

6

7

8

9

0

1

2

3

4

5

6

7

8

9

0

1

2

3

4

5

6

7

8

9

0

1

2

3

4

5

6

7

8

9

0

1

2

3

4

5

6

7

8

9

0

1

2

3

4

5

6

7

8

9

0

1

2

3

4

5

6

7

8

9

0

1

2

3

4

5

6

7

8

9

0

1

2

3

4

5

6

7

8

9

0

1

2

3

4

5

6

7

8

9

0

1

2

3

4

5

6

7

8

9

0

1

2

3

4

5

6

7

8

9

0

1

2

3

4

5

6

7

8

9

0

1

2

3

4

5

6

7

8

9

0

1

2

3

4

5

6

7

8

9

0

1

2

3

4

5

6

7

8

9

0

1

2

3

4

5

6

7

8

9

0

1

2

3

4

5

6

7

8

9

0

1

2

3

4

5

6

7

8

9

0

1

2

3

4

5

6

7

8

9

0

1

2

3

4

5

6

7

8

9

0

1

2

3

4

5

6

7

8

9

0

1

2

3

4

5

6

7

8

9

0

1

2

3

4

5

6

7

8

9

## X AT GAMMA CONVERSION

HBOOK ID = 18

DATE 82/04/13

NO = 18

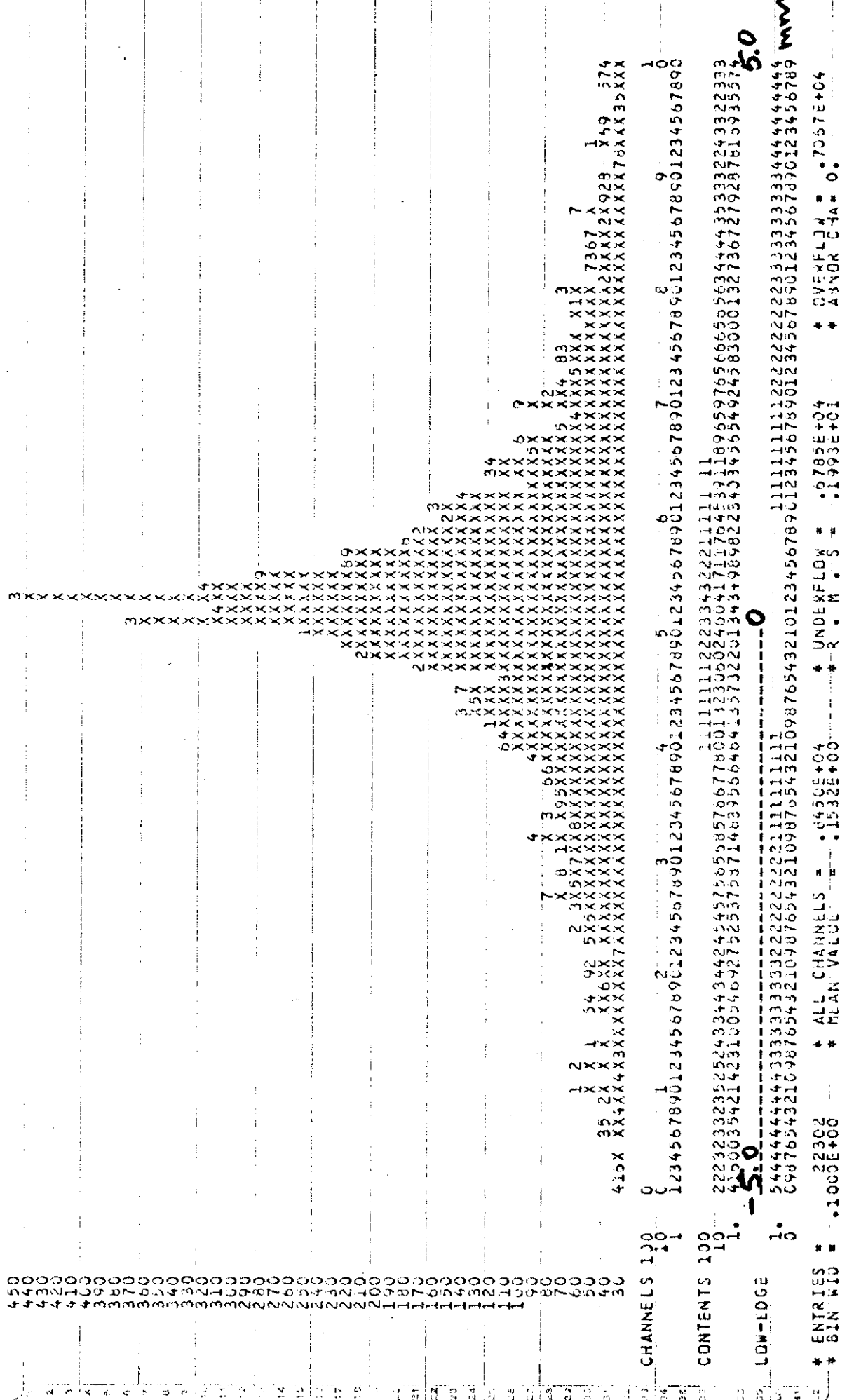


Fig. 24: x - Distribution at gamma conversion



Y AT GAMMA CONVERSION  
HBOOK 10 \* 19

DATE 82/04/13

NO \* 19

360

350

340

330

320

310

300

290

280

270

260

250

240

230

220

210

200

190

180

170

160

150

140

130

120

110

100

90

80

70

60

50

40

30

20

10

0

100

200

300

400

500

600

700

800

900

1000

1100

1200

1300

1400

1500

1600

1700

1800

1900

2000

2100

2200

2300

2400

2500

2600

2700

2800

2900

3000

3100

3200

3300

3400

3500

3600

3700

3800

3900

4000

4100

4200

4300

4400

4500

4600

4700

4800

4900

5000

5100

5200

5300

5400

5500

5600

5700

5800

5900

6000

6100

6200

6300

6400

6500

6600

6700

6800

6900

7000

7100

7200

7300

7400

7500

7600

7700

7800

7900

8000

8100

8200

8300

8400

8500

8600

8700

8800

8900

9000

9100

9200

9300

9400

9500

9600

9700

9800

9900

10000

11000

12000

13000

14000

15000

16000

17000

18000

19000

20000

21000

22000

23000

24000

25000

26000

27000

28000

29000

30000

31000

32000

33000

34000

35000

36000

37000

38000

39000

40000

41000

42000

43000

44000

45000

46000

47000

48000

49000

50000

51000

52000

53000

54000

55000

56000

57000

58000

59000

60000

61000

62000

63000

64000

65000

66000

67000

68000

69000

70000

71000

72000

73000

74000

75000

76000

77000

78000

79000

80000

81000

82000

83000

84000

85000

86000

87000

88000

89000

90000

91000

92000

93000

94000

95000

96000

97000

98000

99000

100000

LOW-EDGE

50

100

150

200

250

300

350

400

450

500

550

600

650

700

750

800

850

900

950

1000

1100

1200

1300

1400

1500

1600

1700

1800

1900

2000

2100

2200

2300

2400

2500

2600

2700

2800

2900

3000

3100

3200

3300

3400

3500

3600

3700

3800

3900

4000

4100

4200

4300

4400

4500

4600

4700

4800

4900

5000

5100

5200

5300

5400

5500

5600

5700

5800

5900

6000

6100

6200

6300

6400

6500

6600

6700

6800

6900

7000

Y' AT GAMMA CONVERSION  
HBOOK ID = 21

DATE 82/04/13 NO \* 21

Y' AT GAMMA CONVERSION	HBOOK ID = 21
144	
145	
146	
147	
148	
149	
150	
151	
152	
153	
154	
155	
156	
157	
158	
159	
160	
161	
162	
163	
164	
165	
166	
167	
168	
169	
170	
171	
172	
173	
174	
175	
176	
177	
178	
179	
180	
181	
182	
183	
184	
185	
186	
187	
188	
189	
190	
191	
192	
193	
194	
195	
196	
197	
198	
199	
200	
201	
202	
203	
204	
205	
206	
207	
208	
209	
210	
211	
212	
213	
214	
215	
216	
217	
218	
219	
220	
221	
222	
223	
224	
225	
226	
227	
228	
229	
230	
231	
232	
233	
234	
235	
236	
237	
238	
239	
240	
241	
242	
243	
244	
245	
246	
247	
248	
249	
250	
251	
252	
253	
254	
255	
256	
257	
258	
259	
260	
261	
262	
263	
264	
265	
266	
267	
268	
269	
270	
271	
272	
273	
274	
275	
276	
277	
278	
279	
280	
281	
282	
283	
284	
285	
286	
287	
288	
289	
290	
291	
292	
293	
294	
295	
296	
297	
298	
299	
300	
301	
302	
303	
304	
305	
306	
307	
308	
309	
310	
311	
312	
313	
314	
315	
316	
317	
318	
319	
320	
321	
322	
323	
324	
325	
326	
327	
328	
329	
330	
331	
332	
333	
334	
335	
336	
337	
338	
339	
340	
341	
342	
343	
344	
345	
346	
347	
348	
349	
350	
351	
352	
353	
354	
355	
356	
357	
358	
359	
360	
361	
362	
363	
364	
365	
366	
367	
368	
369	
370	
371	
372	
373	
374	
375	
376	
377	
378	
379	
380	
381	
382	
383	
384	
385	
386	
387	
388	
389	
390	
391	
392	
393	
394	
395	
396	
397	
398	
399	
400	
401	
402	
403	
404	
405	
406	
407	
408	
409	
410	
411	
412	
413	
414	
415	
416	
417	
418	
419	
420	
421	
422	
423	
424	
425	
426	
427	
428	
429	
430	
431	
432	
433	
434	
435	
436	
437	
438	
439	
440	
441	
442	
443	
444	
445	
446	
447	
448	
449	
450	
451	
452	
453	
454	
455	
456	
457	
458	
459	
460	
461	
462	
463	
464	
465	
466	
467	
468	
469	
470	
471	
472	
473	
474	
475	
476	
477	
478	
479	
480	
481	
482	
483	
484	
485	
486	
487	
488	
489	
490	
491	
492	
493	
494	
495	
496	
497	
498	
499	
500	
501	
502	
503	
504	
505	
506	
507	
508	
509	
510	
511	
512	
513	
514	
515	
516	
517	
518	
519	
520	
521	
522	
523	
524	
525	
526	
527	
528	
529	
530	
531	
532	
533	
534	
535	
536	
537	
538	
539	
540	
541	
542	
543	
544	
545	
546	
547	
548	
549	
550	
551	
552	
553	
554	
555	
556	
557	
558	
559	
560	
561	
562	
563	
564	
565	
566	
567	
568	
569	
570	
571	
572	
573	
574	
575	
576	
577	
578	
579	
580	
581	
582	
583	
584	
585	
586	
587	
588	
589	
590	
591	
592	
593	
594	
595	
596	
597	
598	
599	
600	
601	
602	
603	
604	
605	
606	
607	
608	
609	
610	
611	
612	
613	
614	
615	
616	
617	
618	
619	
620	
621	
622	
623	
624	
625	
626	
627	
628	
629	
630	
631	
632	
633	
634	
635	
636	
637	
638	
639	
640	
641	
642	
643	
644	
645	
646	
647	
648	
649	
650	
651	
652	
653	
654	
655	
656	
657	
658	
659	
660	
661	
662	
663	
664	
665	
666	
667	
668	
669	
670	
671	
672	
673	
674	
675	
676	
677	
678	
679	
680	
681	
682	
683	
684	
685	
686	
687	
688	
689	
690	
691	
692	
693	
694	
695	
696	
697	
698	
699	
700	
701	
702	
703	
704	
705	
706	
707	
708	
709	
710	
711	
712	
713	
714	
715	
716	
717	
718	
719	
720	
721	
722	
723	
724	
725	
726	
727	
728	
729	
730	
731	
732	
733	
734	
735	
736	
737	
738	
739	
740	
741	
742	
743	
744	
745	
746	
747	
748	
749	
750	
751	
752	
753	
754	
755	
756	
757	
758	
759	
760	
761	
762	
763	
764	
765	
766	
767	
768	
769	
770	
771	
772	
773	
774	
775	
776	
777	
778	
779	
780	
781	
782	
783	
784	
785	
786	
787	
788	
789	
790	
791	
792	
793	
794	
795	
796	
797	
798	
799	
800	
801	
802	
803	
804	
805	
806	
807	
808	
809	
810	
811	
812	
813	
814	
815	
816	
817	
818	
819	
820	
821	
822	
823	
824	
825	
826	
827	
828	
829	
830	
831	
832	
833	
834	
835	
836	
837	
838	
839	
840	
841	
842	
843	
844	
845	

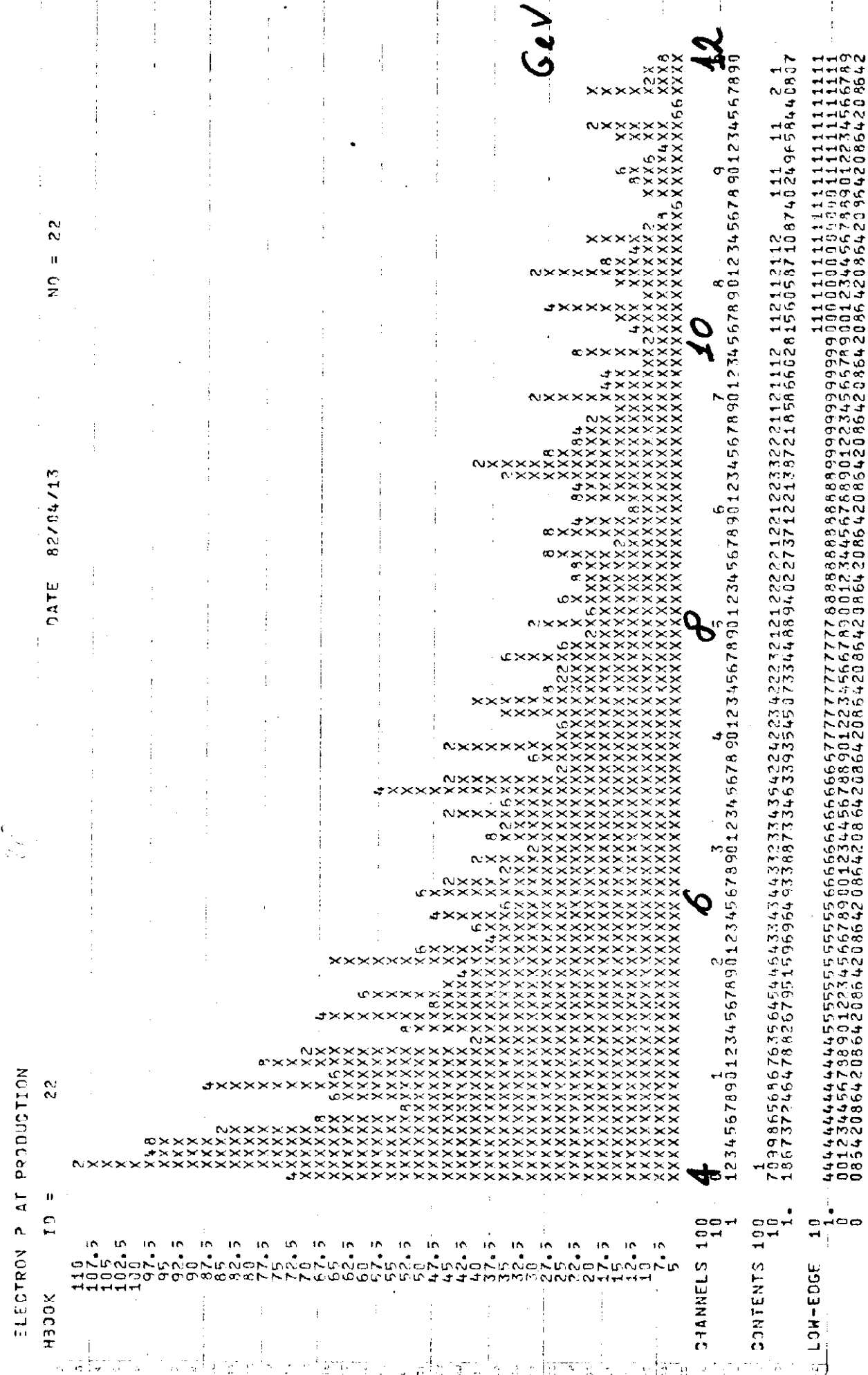


Fig. 28. Momentum Distribution of the Electrons at conversion

POSITRON PA PRODUCTION

DATE 82/04/13 NO = 3E

27

The figure is a scatter plot with the title "GeV" in the top right corner. The x-axis is labeled with values 92, 87, 85, 82, 80, 77, 75, 72, 70, 65, 62, 60, 57, 55, 52, 47, 42, 40, 37, 35, 22, 20, 17, 15, 12, and 9. The y-axis is labeled with values 9, 8, 7, 6, 5, 4, 3, 2, 1, and 0. The data points are represented by 'x' marks. There is a dense cluster of points between x=70 and x=50 and y=8 and y=6. A sparse grid of points extends from x=9 down to x=5 and y=0 down to y=6. Some points are missing, particularly at the lower values.

Fig. 29. Momentum Distribution of the Positions at conversion

S OF E - BREMSSSTR.  
HACK 40 =

23

DATE 62/04/13

NO. \* 23

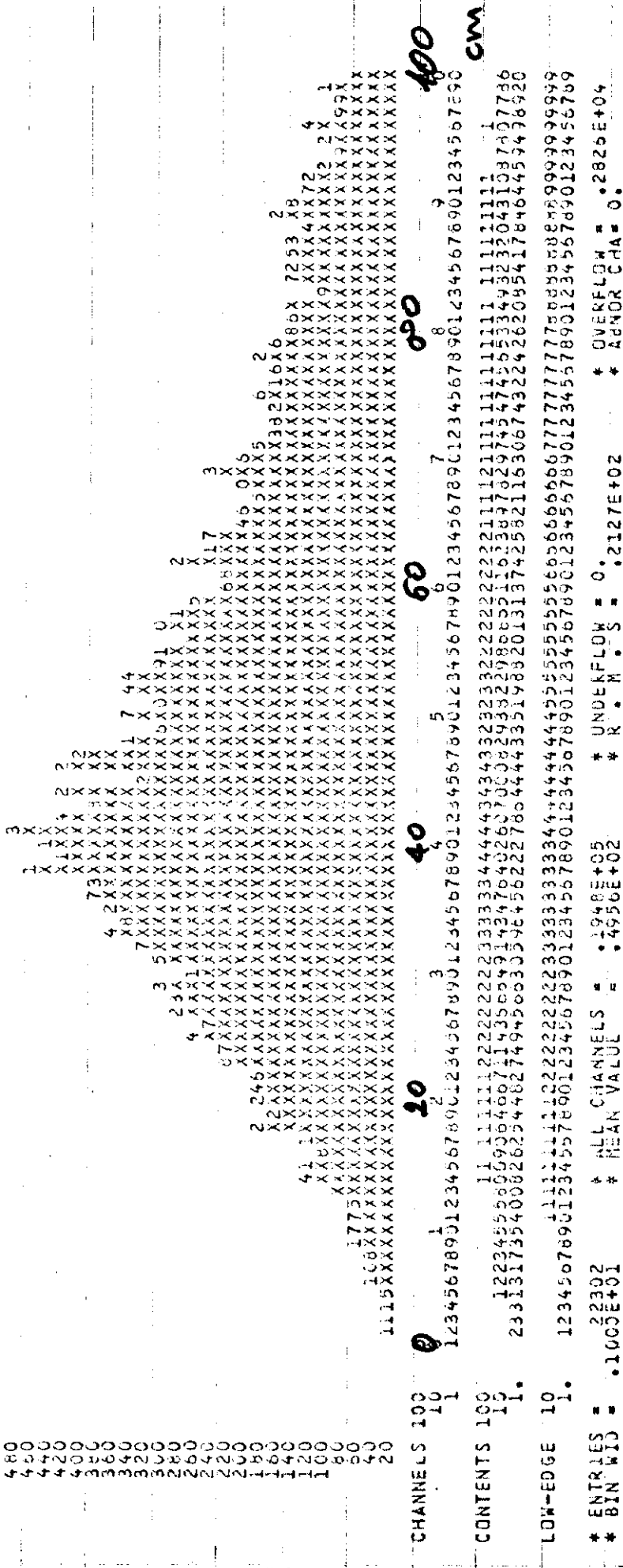


Fig. 30. Distribution of Bremsstrahlung Distances for Electrons

S OF E+ BREMSTK.  
HBOOK 10 =

2

DATE 82/04/13

26



Fig. 31. Distribution of Bremsstrahlung Distances for Positrons

178

FINAL ELECTRON MOMENTUM

卷之三

DATE 82/04/13 NO = 28

DATE 82/04/13

The image shows a large, uniform grid pattern. The grid consists of two types of characters: 'X' and '5'. The 'X' characters are arranged in a staggered, diamond-like pattern across the entire area. Interspersed among these 'X' characters are several '5' characters, which are placed in a more regular, rectangular grid pattern. The overall effect is a repeating, textured pattern.

SCANNING 100

卷之三

卷之三

7 90123456789012345678901234567890

121112221112111211211211111111

41439849165625021072129585957339944673325764

11111111111111111111

卷之三

11 - 4011E105 \* OVERDUE = 00000000

• 2456E+03  
ABNORMAL FLUXES  
• \* \*

卷之三

Fig. 32. Final Momentum Distribution for the Electrons

FINAL POSITRON MOMENTUM 31

DATE 82/04/13 NO 29

DATE 82/04/13

Fig. 33. Final Momentum Distribution for the Positrons

ELECTRON X EMISSION

HADOK ID \* TOT

卷之三

ט' סימן ב

DATE 8/27/04/13

卷之三

CHANNELS    LU U <sup>1</sup> 23436789<sub>1</sub><sup>2</sup> 3456789<sub>2</sub><sup>3</sup> 456789<sub>3</sub><sup>4</sup> 0 A B C D E F G H I J K L M N O P Q R S T U V W X Y Z

\*\*\*  
\*\*\*  
\*\*\*  
\*\*\*  
\*\*\*

34  
• 75  
27  
+ \* \*  
614  
+ 421  
- 233  
---  
32 + 23  
32 + 33  
--- + 42  
32 + 42  
--- 35  
32 + 35  
--- 39  
32 + 39  
--- 42  
32 + 42  
--- 45  
32 + 45  
--- 48  
32 + 48  
--- 51  
32 + 51  
--- 54  
32 + 54  
--- 57  
32 + 57  
--- 60  
32 + 60  
--- 63  
32 + 63  
--- 66  
32 + 66  
--- 69  
32 + 69  
--- 72  
32 + 72  
--- 75  
32 + 75  
--- 78  
32 + 78  
--- 81  
32 + 81  
--- 84  
32 + 84  
--- 87  
32 + 87  
--- 90  
32 + 90  
--- 93  
32 + 93  
--- 96  
32 + 96  
--- 99  
32 + 99  
--- 102

\*\*\*  
12  
• •  
7/10/9  
9  
5  
\*\*\*

\*\*\*

\*\*\*

\*\*\*  
N +  
+ N N  
+ + 0  
0 7 5  
\*\*\*

\*\*\*

111  
H H  
10 9  
10 9  
25 1  
\* \* \*

6:  
593765432169976543210123456789  
-3:0

\* ENTRIES = 46528  
\* SATURATION AT = 31  
\* PLOT = 358 1 3

\*  
\*\*  
\*\*\*  
SCALE = 0.042,3,0.0001ADJ,  
TPE = 1 \* \* \* MINIMUM

卷之三

Fig. 34. Electron Population of the x-x' phase space at the focal plane. All momenta are included

plane. All momenta are included

ELECTRON EMISSION

HANDBOOK OF THE U.S. GOVERNMENT

CANADA

1 N 123456789012345678901234567890 V B

三一八〇

23  
#  
31

Fig. 35. Electron Population

plane. All momenta are included

	PLUT	31	841	31
SATURATION	46520	31		
SCALE	417	3014		401
STEP	1	1		
MINIMUM	31	1	832	31
STATISTICS				

POSIKUN X EMISSION

H300K  
T U \*  
T F O T

DATE

卷之三

Fig. 36. Positron Population

of the  $x-x'$  phase space at the focal plane. All momenta are included

295765432109876543210123456789 -20

```

* ENTRIES = 42228
* SATURATION AT = 3
* SCALE = .1, .2, .3, .4, .5, .6, .7, .8, .9, 1.0
* STEP = 1

```

PL 31 835 31  
358 3567 427  
31 1 822 1 32



ELECTRON X-EM. IN MOM CUT

HBOOK ID = 106

[1] 11228 04/11/2018

二〇  
三一  
九一

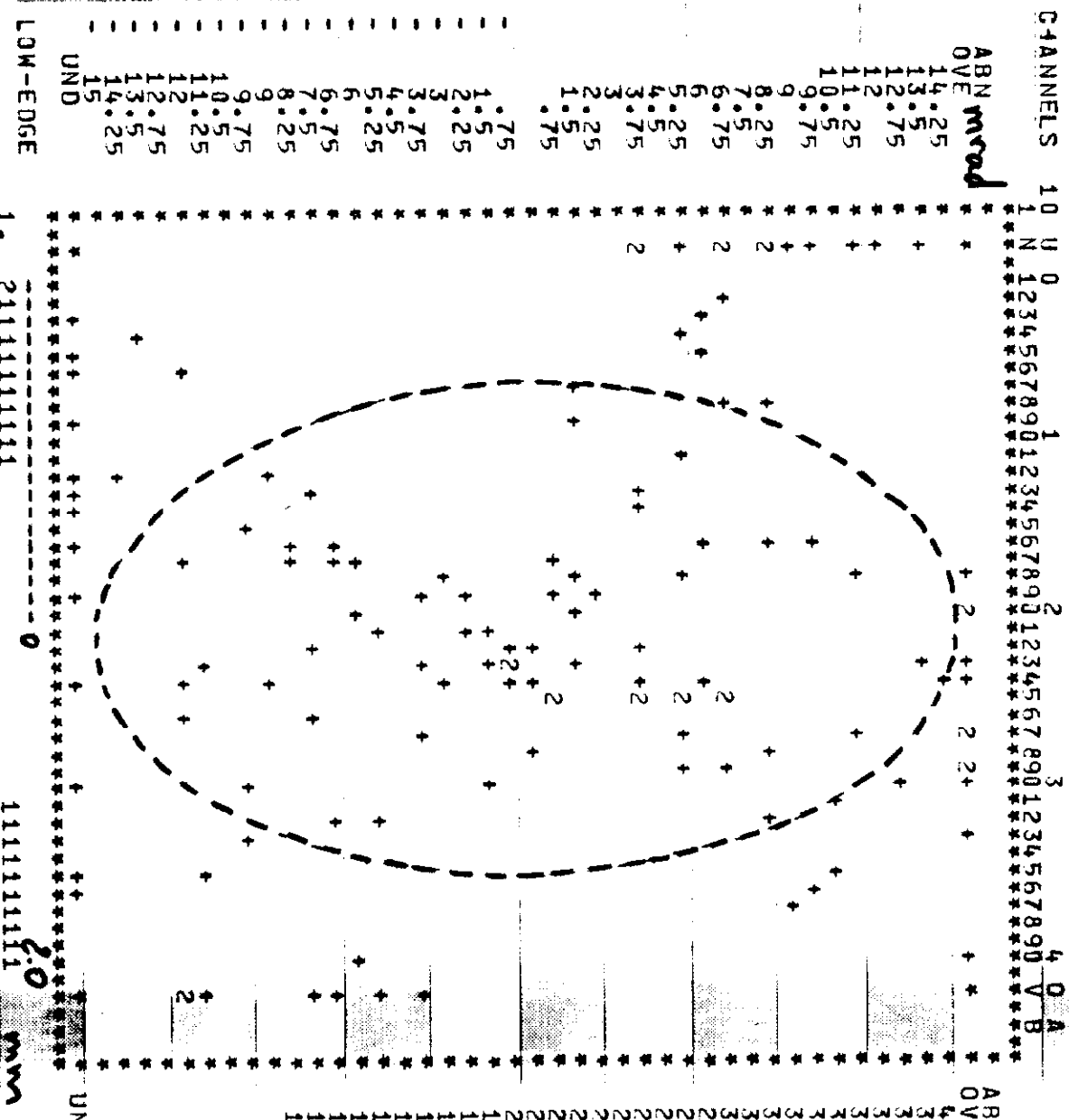


Fig. 38. No. of Electrons (72)

captured within an horizontal accep-

Gitter 01 20

tance of 20 mm-mrad and  $\Delta E/E = \pm 5\%$

ELECTRON Y EM. IN MOM CUT

HBOOK ID = 107

DATE 82/04/13

NO = 36

C CHANNELS 10 U 0 1 2 3 4 5 6 7 8 9 0 1 2 3 4 5 6 7 8 9 0 1 2 3 4 5 6 7 8 9 0 V B

ABN mrad

DVE 14.25 13.5 12.75 11.25 10.5 9.75 8.25 7.5 6.75 6.25 5.25 4.5 3.75 2.25 1.5 1.25 1.5 1.75 2.5 3.75 4.5 5.25 6.75 7.5 8.25 9.75 10.5 11.25 12.75 13.5 14.25 15.0 UND

ABN DVE 40 39 38 37 36 35 34 33 32 31 30 29 28 27 26 25 24 23 22 21 20 19 18 17 16 15 14 13 12 11 10 9 8 7 6 5 4 3 2 1 UND

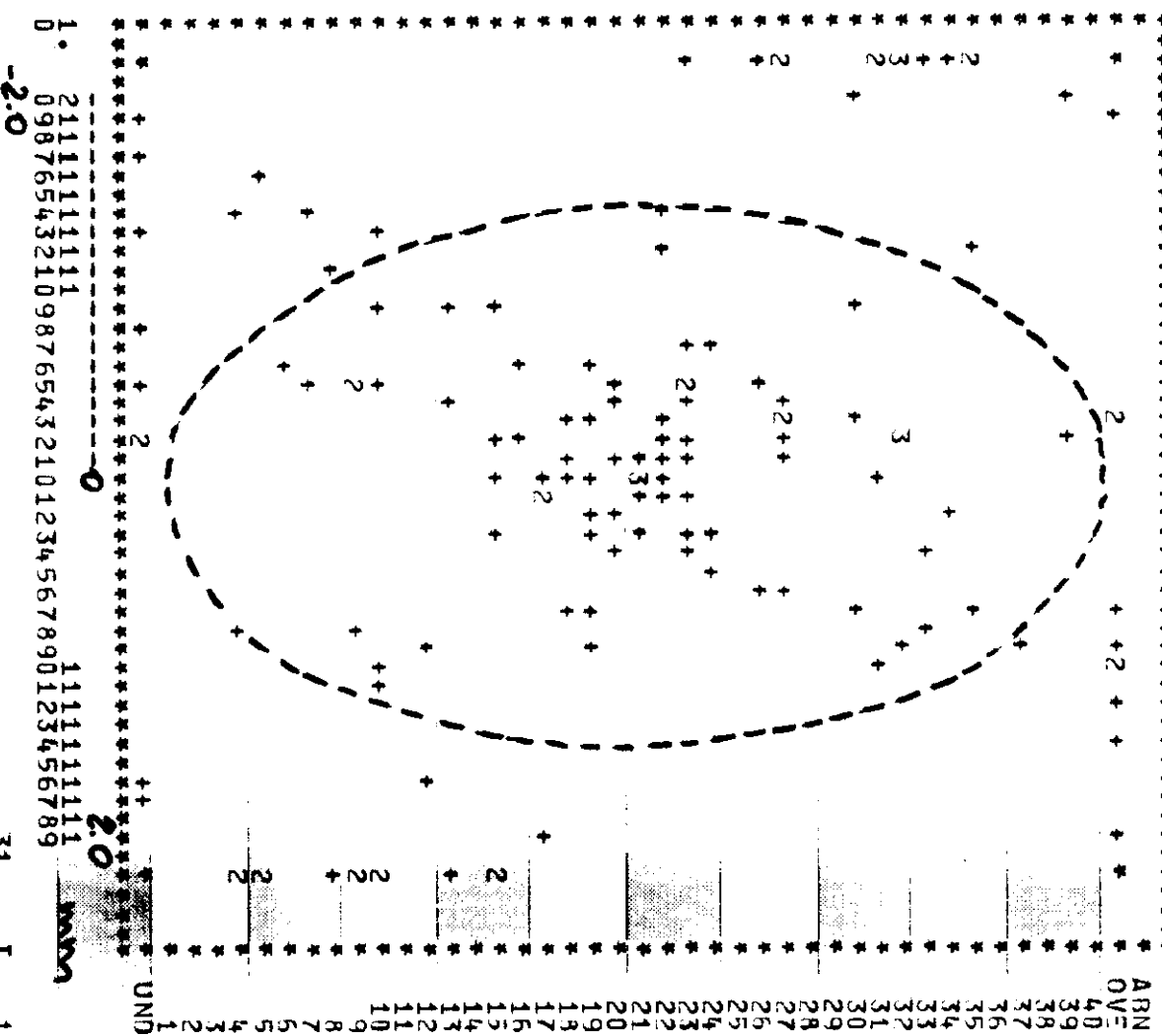


Fig. 39. No. of Electrons (84)  
captured within a vertical acceptance  
of 20  $\pi$  mm-mrad and  $\Delta E/E = \pm 5\%$   
around 5 GeV

\* ENTRIES = 301  
\* SATURATION AT = 31  
\* SCALE = 1, 2, 3, ..., MINIMUM = 0  
\* STFP =

PLOT STATISTICS

31 1 10 1 31  
13 1 96 1 12  
31 1 9 1 31





Fig. 42. No. of Electrons (69)  
 captured within an horizontal acceptance  
 of  $20 \pi$  mrad and  $\Delta E/E = \pm 5\%$   
 around 10 GeV

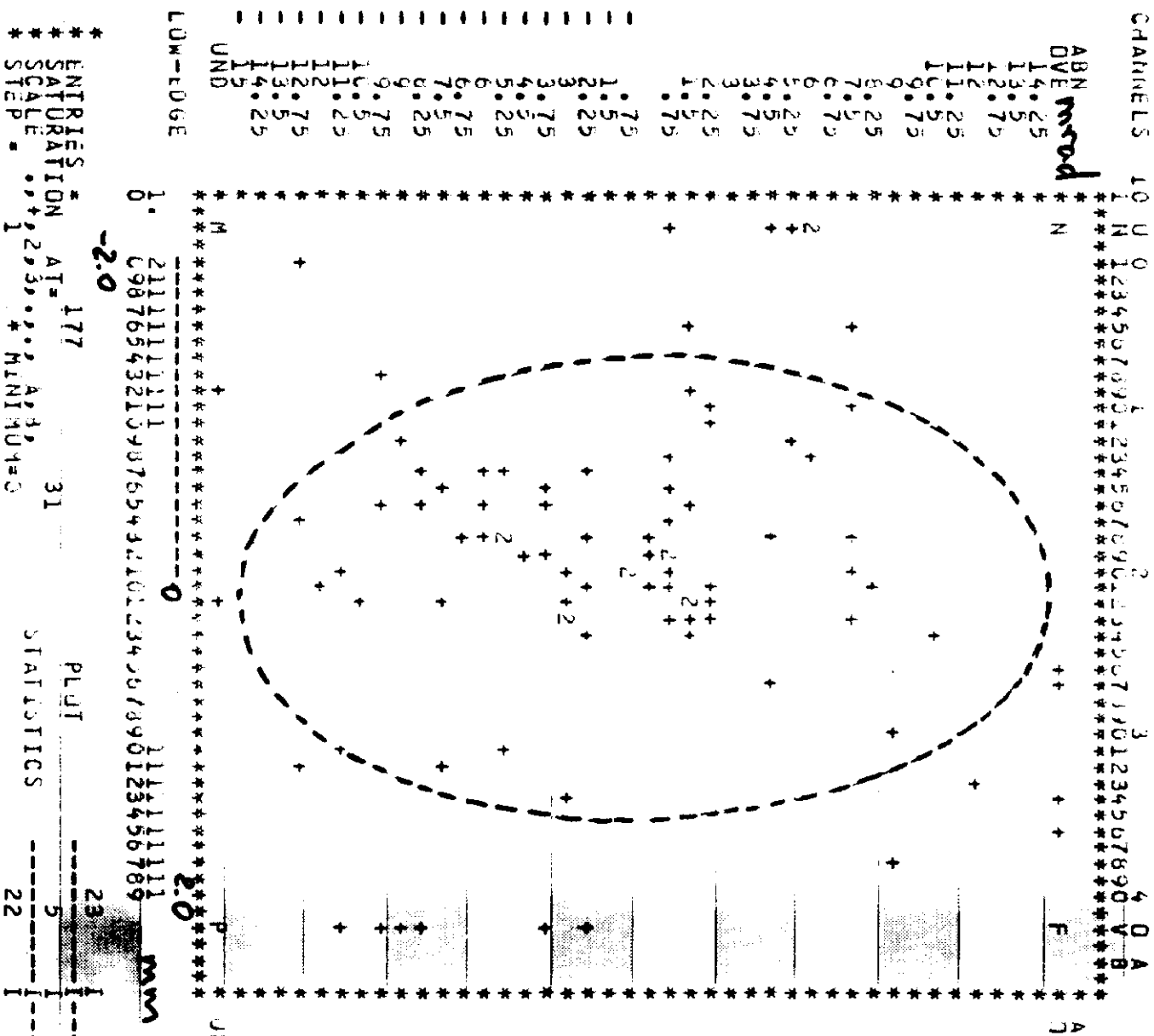


Fig.43. No. of Electrons (68)  
captured within a vertical acceptance  
of 20 mrad and  $\Delta E/E = \pm 5\%$   
around 10 GeV



